DETERMINATION OF ACCURATE MACHINE-SETTINGS FOR THE FACE-MILLING OF HYPOID GEAR

M. Wasif[1,*], M. Rababah[2], S.M. Hasan[1] and S.A. Iqbal[1]
[1]Department of Industrial & Manufacturing Engineering, NED University of Engineering & Technology, Karachi, Pakistan.
[2]Mechanical Engineering Department, Hashemite University, Zarqa, Jordan.

[*]Corresponding author. Tel.: +9221-992616261-8 Ext. 2462; fax: +9221-99261255
E-mail address: wasif@neduet.edu.pk (M. Wasif)

ABSTRACT

A mathematical model for the machine settings of hypoid gears is developed, which is based on accurate blade geometries of a face-milling cutter system. Blades of the cutter system considered in this research, includes rake and relief angles, which are necessary for the efficient metal cutting.
In this research, cutter system orientation on the gear root tangent plane is determined by the root angle, which is calculated for the given spiral angle at the mean point projection of the gear teeth. Whereas, for the position of the cutter system and the gear blank, the tangency between the cutter sweep envelope and the gear teeth at the mean point projection are considered. Considering the tangency and common geometrical entities, a machine reference system is developed.

Keywords: hypoid gears; machine settings; face milling; accurate blade

1 INTRODUCTION

In face milling of hypoid gears, the gear tooth surface is formed by the sweep envelope of the rotating cutter head, which is fed perpendicular to the root cone of the gear blank. In face milling of hypoid gears, the tooth surface is complimentary copy of the cutter sweep surface [1]. Since the gear tooth is the copy of cutter sweep envelope; gear tooth forms the same unit normal and the principal directions as that of the cutter sweep surface as shown in the Fig. 1.

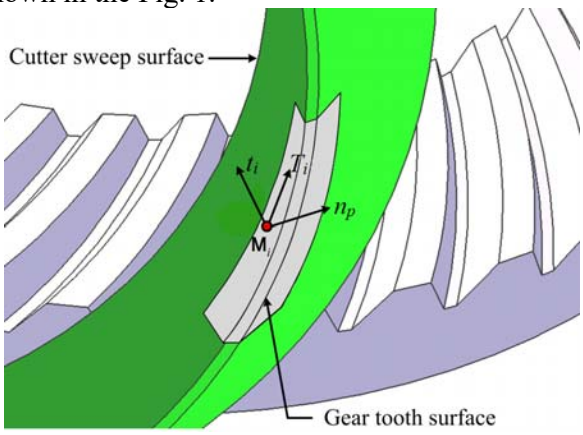

Figure 1. Gear tooth engagement with the cutter sweep envelope during the FORMAT machining

Cutter head of the face milling process contains several groups of inside and outside blades. These blades are arranged to machine the convex and the concave sides of the gear tooth, with the prescribed land width as shown in the Fig. 2.

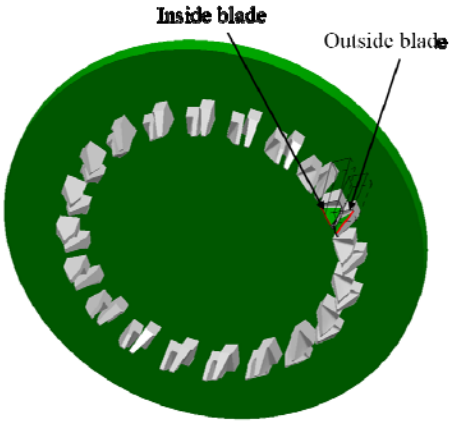

Figure 2. Cutter head assembly containing inside and outside blades

The location and position of the cutter system and the gear blank in the machine reference system are defined by the five geometric parameters called machine settings. Machine settings of the hypoid gear and pinion are based on the cutter system and the gear teeth specifications, which are known for the determination of the machine settings. Since

machine settings are based on the cutter system and gear geometry, therefore, the gear and cutter system geometries are defined in following sections and then the machine settings are discussed and explained in section 4.

Several researches have been published to determine the accurate machine settings.

Litvin presented the machine setting settings for the FORMATE® and the Helixform® Methods, using the tilted cutter head and the local syntheses method [1-2]; Litvin also proposed the cutter tilt mechanism and the machine-setting model [3]. Krezner proposed the computer aided corrections in the machine-setting, based on the first order surface deviations, and claimed that the second order surface deviations are minor [4]. Gosselin et al. proposed the correction methods in machine setting based on the tooth contact analysis (TCA) and performed the numerical regression method until satisfactory machine setting achieved [5-7]. Simon proposed an algorithm to calculate the machine setting corrections to reduce the sensitivity of the gear pair misalignments; moreover, equivalent machine settings for the universal hypoid generator are also calculated [8-11]. Perez et al. presented the analytical method for the determination of machine settings of the bevel gears based on three different geometry of the gear [12].

In gear machining industry, basic machine settings are calculated using the gear cutter and the gear tooth geometry, pilot gears are produced, and then corrected machine settings are calculated based on the surface deviation between the theoretical and the machined gear surfaces [5-7]. Deviations between the theoretical and machined surfaces exist due to the errors caused by the modelling approximation of the teeth surfaces [13].

In the previous research, simplified blade models in cutter systems are considered, in which rake and relief angles of the blades are neglected. The side cutting edge of the blade is assumed to be laid on the normal plane of the cutter [1-3]. Whereas, in the practical gear machining, the top and the side cutting edge of the blade lay on the rake plane of the blade [13] and hence it is called accurate blade model in this article.

In current research, mathematical model for the machine settings of hypoid gears produced by the face milling process is presented. The machine settings in this research are based on; accurate blade model of the cutter system and a spiral angle at the mean point projection of the gear tooth. For the given spiral angle at the mean point, root spiral angle on the root cone tangent plane of the gear is calculated, which decides the cutter orientation on that plane. Machine settings are determined, based on the relative position of the gear teeth and the cutter system, tangent to each other at the mean point projection on the driving side of the gear teeth, which bears the largest pressure during the gear meshing. Mean point **M** is located at the middle of the face width, just above the middle of tooth land, at a height h_M equal to the average of gear and pinion dedendums in that plane [14].

Using the cutter and gear engagement at the mean point projection of the gear tooth, the machine centre is introduced in the system, which lies at the point of intersection of the gear rotation axis and cutter face plane.

This article consists of six sections, first section is the preamble of this research article, second section described the geometry of the cutter sweep envelop and the gear. It includes the relationship between the two geometries. Next two sections address the mathematical model for the root spiral angle at the mean point and the machine setting of hypoid gears. Numerical results and the comparison between the previous and the current research are discussed in the last two sections.

2 GEAR TOOTH AND CUTTER SYSTEM GEOMETRIES

Consider the mean normal cross-section of the gear tooth, located at the middle of the face width. It is defined by the unit normal n_p , and the principal direction t_i along the tooth height, at a point $\mathbf{M}_i$ on the tooth, as shown in the Fig. 3(a). This cross section is called “gear tooth profile”.

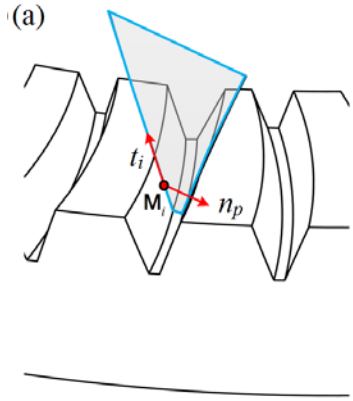

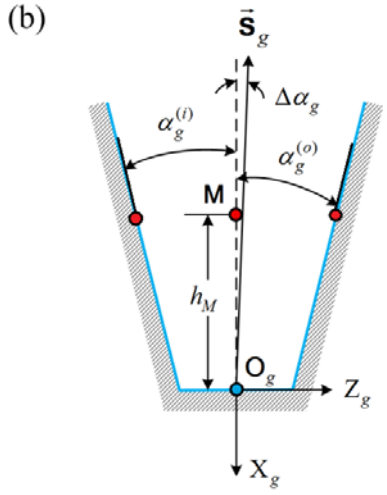

Figure 3. (a) Mean normal cross-section, (b) gear tooth profile

In this profile, consider a coordinate system $\mathbf{O}_g$, attached at the middle of the tooth land, such that the X_gZ_g - plane coincide with the gear tooth profile, where, X_g-axis is perpendicular to the land at $\mathbf{O}_g$, as shown in the Fig. 3(b).

The point **M** lies along the negative X_g-axis at a height h_M as shown in the Figure 3(b).

The flank of the gear tooth formed by the accurate blades in the cutter system are hyperbolic profile rather than straight as assumed in the previous researches. Therefore, the angle between the tangents on the tooth flank at the height h_M and the X_g-axis are called flank angles α_g, as shown in the Figure 3(b). Where, superscripts *(i)* and *(o)* denote the flank angles of the convex and concave sides of the gear teeth.

From the research [13], unit parametric representation of the side cutting edge of the inside and outside blade are given as the function of blade angle α_b, back rake angle α_o, side rake angle α_f, and relief angles γ_f, which is mathematically given by;

$$\overrightarrow{\mathbf{SCE}}_k\left(u_k,\alpha_o^{(k)},\alpha_b^{(k)},\alpha_f^{(k)},\gamma_f^{(k)}\right)=u_k.\overrightarrow{\mathbf{sce}}_k \qquad (1)$$

Where, k can be replaced with either i or o to mention these parameters for the inside or outside blade respectively, u_k be the parameter of the side cutting edges.

Arrangement of inside and outside blade coordinate systems ($O_b^{(i)}$ and $O_b^{(o)}$) are shown in Fig. 4.

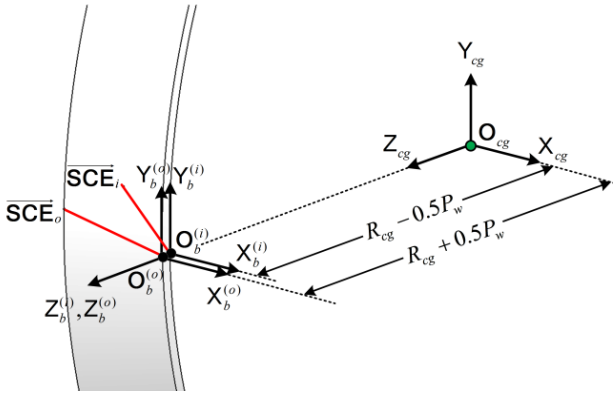

Figure 4. Cutter sweep envelope.

Introducing a cutter head coordinate system O_{cg} which is rigidly attached with the centre face of the cutter head, X_{cg}-axis of the cutter is the roatation axis. O_{cg} have all axes parallel to the $O_b^{(i)}$ coordinate system and is located along negative $Z_b^{(i)}$ axis at a distance, equal to the inside point radius $R_{cg}-0.5P_w$, where R_{cg} is the average cutter radius, measured from the centre of point width P_w to the point O_{cg}. Cutter sweep envelope is formed by revolving the side cutting edges $\overrightarrow{\mathbf{SCE}}_k$ of the blades about the X_{cg}-axis of the cutter, as shown in the Fig. 4. Mathematically, the cutter sweep surface is given by;

$$\vec{\mathbf{S}}_k^{cg}\left(u_k,\theta_{cg}\right) = \mathrm{Rot}\left(X_{cg},\theta_{cg}\right).\mathrm{Tr}\left(Z_b,R_{cg}\mp 0.5P_w\right).\overrightarrow{\mathbf{SCE}}_k \qquad (2)$$

Where, θ_{cg} be the angular parameter of the cutter sweep surfaces. Intersection between the cutter sweep surfaces and the $X_{cg}Y_{cg}$ - plane of the cutter, provides two sets of coordinates $\mathbf{P}_i^{cg}(u_i,\theta_{cg})$ and $\mathbf{P}_o^{cg}(u_o,\theta_{cg})$, which can be generally represented as $\mathbf{P}_k^{cg}(u_k,\theta_{cg})$. Using the least square B-spline regression, cubic B-spline curves are fitted on each set of coordinates with the knot vector $\vec{\mathbf{U}}_k$, where knot vector is generated by average sum method. The curves, fitted on the intersection points of the cutter sweep surfaces are called *equivalent cutting edges* or simply *ECE*, which are shown in the Fig. 5. These *ECEs* are denoted by $\vec{\mathbf{P}}_k^{cg}(v_k)$, where v_k be the B-spline parameters and are bounded within the knot vector.

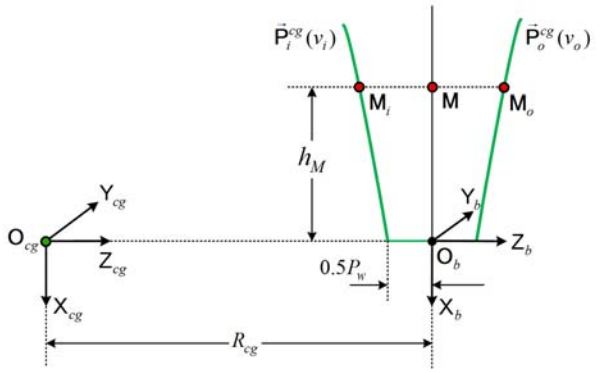

Figure 5. *ECE* in cutter coordinate system

Coordinates of the mean point **M** in cutter coordinate system O_{cg} is given by;

$$\mathbf{M}^{cg} = \begin{bmatrix} -h_M & 0 & R_{cg} & 1 \end{bmatrix}^T \tag{3}$$

Consider another coordinate system $\mathbf{O}_b$, which is attached at the centre of the point width, having same orientation as that of cutter coordinate system as shown in the Figure 5. To develop mathematical expression for the spiral angle at the point $\mathbf{M}_i$, it is desired to calculate the coordinates of mean point projections $\mathbf{M}_k$ on the inside and the outside *ECE*. Therefore, transforming *ECEs* from cutter coordinate system to the $\mathbf{O}_b$ coordinate system. Mathematically, the ECE in $\mathbf{O}_b$ coordinate system are given by;

$$\vec{\mathbf{P}}_k^b = \mathbf{M}_{b,cg} . \vec{\mathbf{P}}_k^{cg} = \mathrm{Tr}\left(Z_{cg}, -R_{cg}\right) . \vec{\mathbf{P}}_k^{cg} \tag{4}$$

The points $\mathbf{M}_k$ on the ECE are calculated by taking the x-components of the ECE equal to the mean height, which determines the parameter v_k. The parameters are then substituted into the B-splines equation to calculate the z-components of the curves. Mathematically, the mean point projections are given by;

$$\begin{aligned} \mathbf{M}_k &= \vec{\mathbf{P}}_k^b \left(v_k^M\right) \\ &= \begin{bmatrix} \mathbf{x}\left(v_k^M\right) & 0 & \mathbf{z}\left(v_k^M\right) & 1 \end{bmatrix}^T \\ &= \begin{bmatrix} -h_M & 0 & \mathbf{z}\left(v_k^M\right) & 1 \end{bmatrix}^T \end{aligned} \tag{5}$$

3 ROOT SPIRAL ANGLE

As mentioned above, the spiral angle β_i controls the curvature of the gear teeth. It is necessary to provide appropriate spiral angle on the driving tooth of the gear for smooth and noiseless operation. Spiral angle is defined on the driving teeth at a height of h_M from the land. It is the angle between the pitch cone generatrix to the point $\mathbf{M}_i$ and the unit normal n_p as shown in the figure 6. On the other hand, root spiral angle defines the orientation of cutter on the gear root cone tangent plane. It is the angle between the root cone generatrix at the point $\mathbf{O}_g$ and the unit normal n_p as shown in the figure 6. For the desired spiral angle β_i, the cutter orientation or root spiral angle β_r is to be calculated.

To acquire the desired shape of the gear teeth, it is required to align the *ECE* with the gear tooth cross section such that the coordinate systems $\mathbf{O}_b$ and $\mathbf{O}_g$ and the symmetric axis are coincided [1] as shown in Figure 7.

The root spiral angle is calculated using an iterated way. Therefore, these two spiral angles can be related as;

$$\beta_i = f(\beta_r) \tag{6}$$

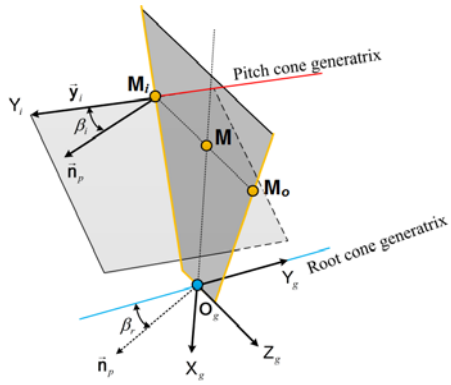

Figure 6. Relationship between the spiral angle at a point, and the root spiral angle

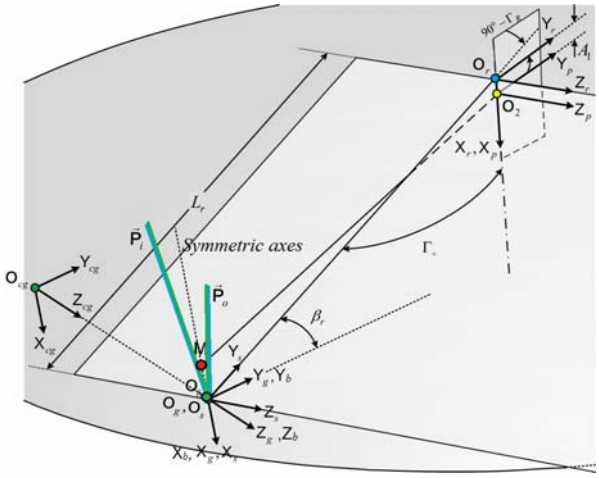

Figure 7. Root spiral angle

Due to the unavailability of the blades, cutter head is titled with an anlge of θ_g about the Y_b axis (case 2) to coincide the symmetric axes of the cutter sweep profile with the gear teeth profile.

To build the relationship between the two spiral angles, it is necessary to relate the pitch cone generatrix, root cone generatrix and unit normal n_p in a single coordinate system. Therefore, the relationship is built by transformation from the $\mathbf{O}_b$ coordinate system to the $\mathbf{O}_2$ coordinate system.

Cutter head is rotated with an angle of β_r about the X_g axis, it from a new coordinate system $\mathbf{O}_s$, as shown in the Figure 7. Where, the Y_s axis forms the generatrix of the root cone, and the X_s axis is parallel to X_g axis. Apex of the root cone $\mathbf{O}_r$ lies at a distance of L_r from the $\mathbf{O}_s$ along the Y_s axis. The orientation of root cone coordinate system $\mathbf{O}_r$ form an angle of $90^\circ - \Gamma_R$ about the Z_r axis. The X_r axis of the coordinate system $\mathbf{O}_r$ is directed along the gear rotation axis, where Γ_R be the root angle as shown in Figure 7. Pitch cone coordinate system $\mathbf{O}_2$ lies at a distance of A_1 along the X_r axis, having same orientation as $\mathbf{O}_r$. Distances L_r and A_1 are determined by the AGMA standards [16].

The vectors n_p and $\mathbf{M}_i$ are transformed to the coordinate system $\mathbf{O}_2$.

$$\vec{n}_p^2 = \mathbf{M}_{2,g}.\vec{n}_p^g \tag{7}$$

$$\mathbf{M}_i^2 = \mathbf{M}_{2,g}.\mathbf{M}_{g,b}.\mathbf{M}_i \tag{8}$$

Transformation from $\mathbf{O}_g$ to the $\mathbf{O}_2$ is mathematically given by;

$$\mathbf{M}_{2,g} = \mathrm{Tr}(\mathsf{Z}_r, -A_1).\mathrm{Rot}(\mathsf{Z}_s, 90^\circ - \Gamma_R). \mathrm{Tr}(\mathsf{Y}_s, -L_r).\mathrm{Rot}(\mathsf{X}_g, \beta_r) \tag{9}$$

$$\mathbf{M}_{g,b} = \mathrm{Rot}(\mathsf{Y}_b, \theta_g).\mathrm{Tr}(\mathsf{X}_g, a).\mathrm{Tr}(\mathsf{Z}_g, b) \tag{10}$$

Where, θ_g be the tilt angle of the cutter, whereas, a and b be the tilt corrections (case 2), as discussed in the previous article [14]. For the exact cutter head with out tile (case 1), $\mathbf{M}_{g,b}$ is a unity matrix.

A unit vector y_i, emerging from the pitch cone generatrix $\mathbf{O}_2$ to the point $\mathbf{M}_i$ is considered, as shown in the Figure 6.

Therefore, the spiral angle at this point is given by,

$$\beta_i = \cos^{-1}\left(\vec{\mathbf{n}}_p.\vec{\mathbf{y}}_i\right) \tag{11}$$

Single variable optimization is used to calculate the root spiral angle for the given spiral angle at the driving mean point projection, which is shown in the Figure 7.

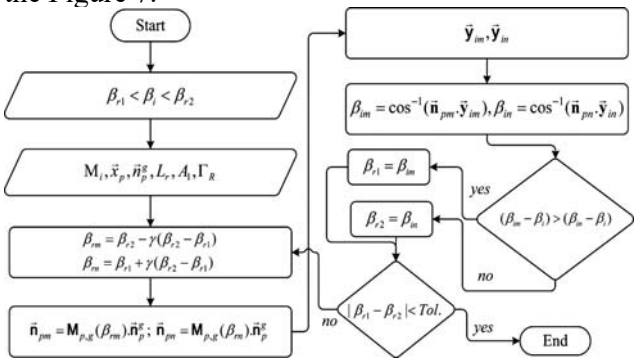

Figure 7. Algorithm for the root spiral angle

Initial guess values of the β_r are provided around the given value of β_i, the optimization parameters are calculated, cutter is rotated about the X_g axis with these angles, and all the equations from equations 7 to 11 are calculated. If equation 11 provides the spiral angle equal to the given spiral angle within the specified tolerance, the algorithm saves the value of β_r as the final value, otherwise, the parameters are re-calculated, and the iterations are performed, until the defined criteria is reached.

4 MACHINE SETTINGS

The machine settings for the face milling of hypoid gears are calculated in the machine coordinate system $\mathbf{O}_m$. These machine settings parameters, with the cutter and gear coordinate systems are shown in the Figure 9.

Consider a unit vector $\vec{\mathbf{p}}_w$ along the point width of the cutter. A point on this vector is given by $\mathbf{P}_w^b = \begin{bmatrix}0 & 0 & 1\end{bmatrix}^T$. Coordinates of a point along the unit normal n_p is given by $\mathbf{N}_p^b = \begin{bmatrix}0 & 1 & 0\end{bmatrix}^T$. Coordinates of another point along the gear rotation axis in the coordinate system is presented as $\mathbf{X}_p^2 = \begin{bmatrix}1 & 0 & 0\end{bmatrix}^T$.

There are three displacements and two angular machine settings are to be calculated as shown in the Figure 8.

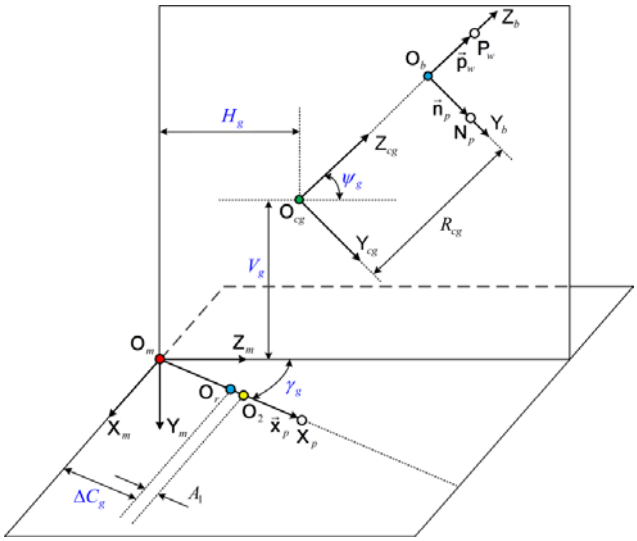

Figure 9. Machine settings for the face milling of hypoid gear

Transforming the coordinates of all origins and mentioned vectors in the pitch cone coordinate system $\mathbf{O}_2$.

$$\mathbf{O}_b^2 = \mathbf{M}_{2,g}.\mathbf{M}_{g,b}.\begin{bmatrix}0 & 0 & 0 & 1\end{bmatrix}^T \tag{12}$$

$$\mathbf{O}_r^2 = \mathbf{M}_{2,r}.\begin{bmatrix}0 & 0 & 0 & 1\end{bmatrix}^T \tag{13}$$

$$\mathbf{O}_{cg}^2 = \mathbf{M}_{2,cg}.\begin{bmatrix}0 & 0 & 0 & 1\end{bmatrix}^T \tag{14}$$

$$\mathbf{P}_w^2 = \mathbf{M}_{2,cg}.\mathbf{P}_w^b \tag{15}$$

$$\mathbf{N}_p^2 = \mathbf{M}_{2,cg}.\mathbf{N}_p^b \tag{16}$$

Origin of the machine coordinate system $\mathbf{O}_m$ is defined as the machine centre, and shown in the Figure 9. It is located at the intersection of the vector along gear rotation axis $\vec{\mathbf{x}}_p$ and the plane formed by the vectors $\vec{\mathbf{p}}_w$ and $\vec{\mathbf{n}}_p$, which is called machine plane. Therefore, the equation of the gear rotation axis and the $\mathsf{Y}_b\mathsf{Z}_b$ plane is given by,

$$\mathsf{L}(t) = (1-t).\mathbf{O}_r^2 + t.\mathbf{X}_p^2 \tag{17}$$

$$\mathsf{P}(u,v) = \mathbf{O}_b^2 + u.\left(\mathbf{P}_w^2 - \mathbf{O}_b^2\right) + v.\left(-\mathsf{N}_p^2 - \mathbf{O}_b^2\right) \tag{18}$$

Where t is the parameter of the line $\mathsf{L}(t)$ along the gear rotation axis, and the parameters u and v belongs to the machine plane. Point of intersection between the line $\mathsf{L}(t)$ and the plane $\mathsf{P}(u,v)$ is evaluated by the relation;

$$\mathsf{L}(t_m) = \mathsf{P}(u_m, v_m) \tag{19}$$

It provides the parameters as the solution, for the machine centre. Parameter t_m represents the distance between the apex of the root cone $\mathbf{O}_r$ and the machine centre $\mathbf{O}_m$, which is called withdraw from the machine plane, and denoted by ΔC_g, Therefore, mathematically the it is calculated by;

$$\Delta C_g = \sqrt{\left(\mathsf{L}_x(t_m)\right)^2 + \left(\mathsf{L}_y(t_m)\right)^2 + \left(\mathsf{L}_z(t_m)\right)^2} \tag{20}$$

Therefore, the machine centre $\mathbf{O}_m$ in the coordinate system $\mathbf{O}_r$ is represented by $\mathbf{O}_m^r = \begin{bmatrix}\Delta C_g & 0 & 0\end{bmatrix}^T$.

The displacement ΔC_g defines the location of the root cone apex in machine reference system, which cannot be located in the gear blank. Therefore, location of the face cone apex $\mathbf{O}_f$ is calculated in the machine coordinate system by the displacement ΔX_g [13], which is mathematically given by;

$$\Delta X_g = \Delta C_g + d_k + A_1 \tag{21}$$

Where d_k be the distance between the pitch cone apex and the face cone apex. Direction of the X_m axis is defined by a vector x_m, which is perpendicular to the machine plane. The normal to the plane formed by the vectors x_m and x_p specifies the direction of the Y_m axis, which is represented by the vector y_m, whereas Z_m axis is perpendicular to the $\mathsf{X}_m\mathsf{Y}_m$ plane. Direction vectors of the machine coordinate system are given by;

$$\vec{\mathbf{X}}_m^p = x_m + \mathbf{O}_m^r = \frac{\vec{\mathbf{n}}_p \times \vec{\mathbf{p}}_w^p}{\left|\vec{\mathbf{n}}_p \times \vec{\mathbf{p}}_w^p\right|} + \mathbf{O}_m^r \tag{22}$$

$$\vec{\mathbf{Y}}_m^p = y_m + \mathbf{O}_m^r = \frac{\vec{\mathbf{x}}_p \times \vec{\mathbf{x}}_m^p}{\left|\vec{\mathbf{x}}_p \times \vec{\mathbf{x}}_m^p\right|} + \mathbf{O}_m^r \tag{23}$$

$$\vec{\mathbf{Z}}_m^p = z_m + \mathbf{O}_m^r = \frac{\vec{\mathbf{x}}_m^p \times \vec{\mathbf{y}}_m^p}{\left|\vec{\mathbf{x}}_m^p \times \vec{\mathbf{y}}_m^p\right|} + \mathbf{O}_m^r \tag{24}$$

An angular machine setting, which measures the angle between the machine plane and the gear rotation axis, it is called machine root angle (γ_g). It is mathematically given by;

$$\gamma_g = \cos^{-1}\left(\vec{\mathbf{x}}_p . \vec{\mathbf{z}}_m^p\right) \tag{25}$$

Another angular machine setting is called machine spiral angle (ψ_g), it is the angle between the cutter tilt plane $\mathsf{X}_{cg}\mathsf{Z}_{cg}$ and the Z_m axis, it is given by;

$$\psi_g = \frac{\pi}{2} - \cos^{-1}\left(\vec{\mathbf{y}}_m^p . \vec{\mathbf{p}}_w^p\right) \tag{26}$$

The location of the cutter coordinate system $\mathbf{O}_{cg}$ in machine coordinate system is defined by the displacements H_g and V_g along the Z_m and Y_m axes respectively. Mathematically these machine settings are given by;

$$H_g = \frac{\left|\left(\mathbf{O}_c^p - \mathbf{O}_m^p\right) \times \left(\mathbf{O}_c^p - \mathbf{Z}_m^p\right)\right|}{\left|\mathbf{Z}_m^p - \mathbf{O}_m^p\right|} \tag{27}$$

$$V_g = \pm \frac{\left|\left(\mathbf{O}_c^p - \mathbf{O}_m^p\right) \times \left(\mathbf{O}_c^p - \mathbf{Y}_m^p\right)\right|}{\left|\mathbf{Y}_m^p - \mathbf{O}_m^p\right|} \tag{28}$$

Where, '±' signs are for the machining of left hand or right hand direction of the hypoid gear teeth.

5 RESULTS

Machine settings of a hypoid gear is calculated for the given spiral angle at the mean point of the driving side tooth. The data for the inside and outside gear-cutting blades, cutter radius, and the specification of the tooth geometry are taken as input in this algorithm, which are shown in the tables 1 to 4. Table 1 shows the specifications of the hypoid gear cones and teeth, whereas, tables 2 and 3 contains the data of the blade and the cutter for the case I and case II respectively [14]. To compare the result of the previous [7] and current research, machine setting for the simplified and accurate blade models for the case 1 and case 2, along with the auxiliary angle are shown in the tables 4 and 5. Fig. 10 and table 6 illustrate the deviation between the gear teeth surfaces modelled with the machine settings and cutter head of simplified and accurate blade models. It can be seen that these deviation cause the geometric errors in the gear models not only on the heel and toe but also at the mean points of the teeth surface.

Table 1. Specification of hypoid gear

Parameters	Sym.	Convex side	Concave side
Gear flank angle	$\alpha_g^{(k)}$	23°11′0″	21°49′0″
Gear face angle	Γ_o	81°06′0″	
Gear root angle	Γ_R	75°28′0″	
Gear dedendum angle	δ_G	4°54′0″	
Gear pitch point length	L_P	150.9600 mm	
Root to pitch apex	A_1	1.6885 mm	
Face width	F	43.0000 mm	
Spiral angle at $\mathbf{M}_i$	β_i	31°34′12″	

Table 2. Specifications of blade and cutter head parameters for the case I (without cutter tilt).

Parameters	Previous literature [7]		Proposed research	
	Convex side	Concave side	Convex side	Concave side
Back rake angle ($\alpha_o^{(k)}$)	0	0	20°0′0″	20°0′0″
Side rake angle ($\alpha_f^{(k)}$)	0	0	12°0′0″	12°0′0″
Side relief angle ($\gamma_f^{(k)}$)	0	0	10°0′0″	10°0′0″
Blade angle ($\alpha_b^{(k)}$)	23°11′0″	21°49′0″	19°01′14″	16°37′35″
Av. cutter radius (R_{cg})	152.4 mm		152.4 mm	
Point width (P_w)	2.54 mm		2.54 mm	

Table 3. Blade and the cutter head data for the case II (with cutter tilt).

Parameters	Previous literature [7]		Proposed research	
	Convex side	Concave side	Convex side	Concave side
Back rake angle ($\alpha_o^{(k)}$)	0	0	20°0′0″	20°0′0″
Side rake angle ($\alpha_f^{(k)}$)	0	0	12°0′0″	12°0′0″
Side relief angle ($\gamma_f^{(k)}$)	0	0	10°0′0″	10°0′0″
Blade angle ($\alpha_b^{(k)}$)	22°30′0″	22°30′0″	18°22′6″	17°15′39″
Av. cutter radius (R_{cg})	152.4 mm		152.4 mm	
Point width (P_w)	2.54 mm		2.54 mm	
Cutter tilt angle	θ_g		–0°41′0″	
Cutter corrections	a , b		-0.0151 mm, -0.0001 mm	

Table 4. Machine settings of the hypoid gear for case I (without cutter tilt).

Parameter	Previous research [7]		Proposed research	
	Convex side	Concave side	Convex side	Concave side
Root spiral angle (β_r)	32°50′0″		32°50′0″	
Machine root angle (γ_g)	75°28′0″		75°28′0″	
Machine spiral angle (ψ_g)	32°50′0″		32°50′0″	
Machine centre to back correction (ΔX_g)	1.0685 mm		1.0686 mm	
Cutter horizontal setting (H_g)	128.0694 mm		128.0416 mm	
Cutter vertical setting (V_g)	68.3526 mm		68.2009 mm	

Table 5. Machine settings of the hypoid gear for the case II (with cutter tilt).

Parameter	Previous research [7]		Proposed research	
	Convex side	Concave side	Convex side	Concave side
Root spiral angle (β_r)	32°50′0″		32°50′0″	
Machine root angle (γ_g)	75°49′0″		75°49′33″	
Machine spiral angle (ψ_g)	30°34′0″		30°33′40″	
Machine centre to back correction (ΔX_g)	0.0600 mm		0.0619 mm	
Cutter horizontal setting (H_g)	125.1400 mm		125.2552 mm	
Cutter vertical setting (V_g)	73.0300 mm		72.9789 mm	

Table 6. Surface deviations in the gear teeth modelled with the machine settings and cutter head of simplified and accurate blade models.

	Surface Deviation - Case I *(μm)*		Surface Deviation - Case II *(μm)*	
	Convex side	Concave side	Convex side	Concave side
a	168.57	147.30	164.61	99.24
b	153.41	153.83	128.72	128.79
c	143.77	152.43	118.60	129.48
d	149.35	149.71	125.12	125.13
e	178.36	173.98	173.44	167.42

It can be seen from Table 6, that the deviation is maximum at the mean points of the two models which are denoted by “e” in table 6. The mean point is crucial for the contact.

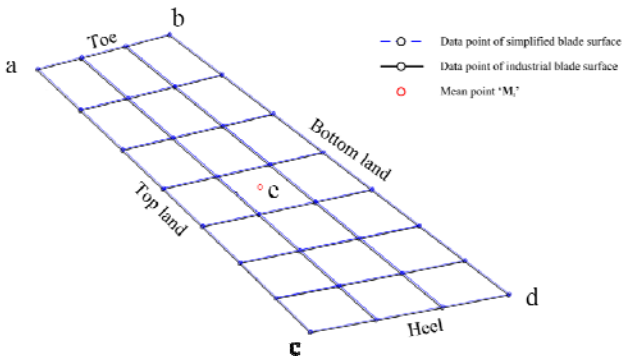

Figure 10. Surface deviations in the gear teeth modelled with the machine settings and cutter head of simplified and accurate blade models

6 CONCLUSION

Results show that the machine settings for the gear teeth modelled with the simplified and the accurate blade model differ, due to reason that the spiral angles at the mean points are different for the same root spiral angle. Machine root angle does not change for in all the examples, since it depends upon the gear cone parameters. It is also observed that the machine settings for the tilted cutter are more sensitive for the rake and relief angles, which also change the machine centre to back setting. The algorithm also covers the cutter tilt corrections, which restrain the cutter to gauge into the root cone, but the corrections cause the change in pitch cone apex for the mean point, which is also overcome in this research.

REFERENCES

[1] F.L. Litvin, Y. Gutman, Method of Synthesis and Analysis for Hypoid Gear-Drives of 'Formate' and 'Helixform'" Part 1, *Journal of Mechanical Design*, 103, 83-88; 1981.

[2] F.L. Litvin, Y. Gutman, Method of Synthesis and Analysis for Hypoid Gear-Drives of 'Formate' and 'Helixform'" Part 2, *Journal of Mechanical Design*, 103, 83-88; 1981.

[3] F. L. Litvin, Y. Zhang, M. Lundy and C. Heine, Determination of Settings of a Tilted Head Cutter for Generation of Hypoid and Spiral Bevel Gears, *Journal of Mechanical Design*, 110, 495-500, 1988.

[4] T. J. Krenzer, Computer aided corrective machine settings for manufacturing bevel and hypoid gear sets, *Technical papers : Fall Technical Meeting*, Washington DC, 1984.

[5] C. Gosselin, Corrective machine settings of spiral-bevel and hypoid gears with profile

deviations, *World Congress on Gearing and Power Transmission*, Paris, 1999.
[6] C. Gosselin, T. Nonaka, Y. Shiono, A. Kubo and T. Tatsuno, Identification of the Machine Settings of Real Hypoid Gear Tooth Surfaces, *Journal of Mechanical Design*, 120, 429-440, 1998.
[7] C. J. Gosselin and L. Cloutier, The Generating Space for Parabolic Motion Error Spiral Bevel Gears Cut by the Gleason Method, *Journal of Mechanical Design*, 115, 483-489, 1993.
[8] V. Simon, Optimal Machine Tool Setting for Hypoid Gears Improving Load Distribution, *Journal of Mechanical Design*, 123, 577-582, 2001.
[9] V. Simon, Advanced Manufacture of Spiral Bevel Gears on CNC Hypoid Generating Machine, *Journal of Mechanical Design*, 132, 031001-1-8, 2010.
[10] V. Simon, Generation of Hypoid Gears on CNC Hypoid Generator, *Journal of Mechanical Design*, 133, 121003-1-9, 2011.
[11] V. Simon, Machine-Tool Settings to Reduce the Sensitivity of Spiral Bevel Gears to Tooth Errors and Misalignments, *Journal of Mechanical Design*, 130, 082603-1-10, 2008.
[12] I. G. Perez, A. Fuentes and K. Hayasaka, Analytical Determination of Basic Machine-Tool Settings for Generation of Spiral Bevel Gears From Blank Data, *Journal of Mechanical Design*, 132, 101002-1-11, 2010.
[13] S. Xie, A genuine face milling cutter geometric model for spiral bevel and hypoid gears, *Journal of Advanced Manufacturing Technology,* 67(9-12), 2619-2616, 2013.
[14] M. Wasif, Z.C. Chen, Cutter radius and blade angle selection model for the high speed face milling of hypoid gear, *International conference on virtual machining process technology*, Montreal, 2011.
[15] AGMA, Design Manual for Bevel Gears, *ANSI/AGMA standards*, USA, 2005.